I&EC research
Industrial & Engineering Chemistry Research

Article

pubs.acs.org/IECR

# Kinetics of Strong Acid Hydrolysis of a Bleached Kraft Pulp for Producing Cellulose Nanocrystals (CNCs)

Qianqian Wang,[†,‡] Xuebing Zhao,*[,‡,§] and J. Y. Zhu*[,‡]

[†]Biofuels Institute, School of the Environment, Jiangsu University, Zhenjiang, China

[§]Institute of Applied Chemistry, Department of Chemical Engineering, Tsinghua University, Beijing, China

[‡]Forest Products Laboratory, USDA Forest Service, Madison, Wisconsin 53726, United States

Supporting Information

**ABSTRACT:** Cellulose nanocrytals (CNCs) are predominantly produced using the traditional strong acid hydrolysis process. In most reported studies, the typical CNC yield is low (approximately 30%) despite process optimization. This study investigated the hydrolysis of a bleached kraft eucalyptus pulp using sulfuric acid between 50 and 64 wt % at temperatures of 35−80 °C over time periods of up to 240 min for the production of CNCs. The experimental design captured the feature of the coexistence of a variety of reaction products, such as CNC, cellulosic solid residue (CSR), glucose, and xylose, in the product stream for accurate kinetic modeling to improve the CNC production yield. The kinetic model describing the solubilization of cellulose fibers used three phenomenological reactions, namely, hydrolysis of xylan to form xylose, depolymerization of cellulose to CNCs, and hydrolysis of cellulose to form glucose, each of which can be described by pseudohomogenous first-order kinetics. The concept of "degrees of hydrolyzable xylan or cellulose" to reflect the inhomogeneity of xylan or cellulose in hydrolysis was incorporated into the kinetic modeling to improve model accuracy. The developed model showed excellent predictability for CNC production. Both the experimental data and the model clearly indicate that CNC production was limited by cellulose depolymerization at low acid concentrations of below 58 wt %, but controlled by CNC degradation when the acid concentration was higher than 58 wt %. This work for the first time provides the most plausible description of CNC production kinetics, which is significant for the commercial production of CNCs.

## INTRODUCTION

Cellulose nanocrystals (CNCs) have been found to exhibit very special mechanical and optical properties.[1−6] CNCs can be used as powerful building blocks for the production of high-quality, durable, lightweight, and cost-effective products for a variety of applications.[7,8] CNCs are mainly produced using the traditional acid hydrolysis method from cellulosic fibers that are renewable and abundant.[6,9−11] When strong sulfuric acid is used, the resultant CNC surface is negatively charged as a result of the formation of sulfate groups and forms a stable colloidal suspension, which is favorable for aqueous processing.[10] However, approximately 70% of the cellulose can be simultaneously hydrolyzed to sugars, resulting in a typical CNC yield of only 30%. The sugars cannot be economically recovered from the strong acid solution, which significantly affects CNC production economics. Several studies were carried out to optimize CNC production but were not able to avoid significant sugar degradation and improve the CNC yield,[12−14] because cellulose depolymerization and sulfation and CNC production occur abruptly and simultaneously.[9,12]

Recently, we discovered a very narrow operating window in which cellulose degradation to sugars can be eliminated, resulting in cellulosic solid residue (CSR), which is easily recoverable, in addition to a high CNC yield of approximately 55%.[9] The CSR also contains sulfate groups, which facilitate nanofibrillation with low energy input to produce cellulose nanofibrils (CNFs) with good optical and mechanical properties.[15] The recovery of CSR in CNC production has significant economic benefits. Developing an understanding of the reaction kinetics of the acid hydrolysis of cellulosic fibers at high acid concentrations can reduce the conversion of cellulose to sugars and facilitate the recovery of CSR and, therefore, has commercial significance. Although the hydrolysis of lignocelluloses under dilute acid conditions has been explored in the literature,[16,17] we are not aware of reported kinetic studies on the hydrolysis of cellulosic materials at very high acid concentrations close to the cellulose solubilization point of 64 wt %. The rapid hydrolysis reactions of cellulosic fibers at high concentrations result in a very narrow operating widow, which creates experimental difficulties in representatively capturing the reaction process as required for accurate modeling. The objective of this work was thus to conduct a kinetic study of the acid hydrolysis of cellulosic fibers for CNC production. The experiments were designed to capture the narrow operating window in which significant amounts of CSR and CNC and small amounts of sugars coexist in the reactant stream. A kinetic model was then developed based on the experimental data as a mathematical tool for large-scale process design.

## MATERIALS AND METHODS

**Materials.** All materials were the same as those described in our previous study.[9] Sulfuric acid of ACS reagent grade was

Received: April 23, 2014
Revised: June 9, 2014
Accepted: June 10, 2014
Published: June 10, 2014





dx.doi.org/10.1021/ie501672m | Ind. Eng. Chem. Res. 2014, 53, 11007−11014

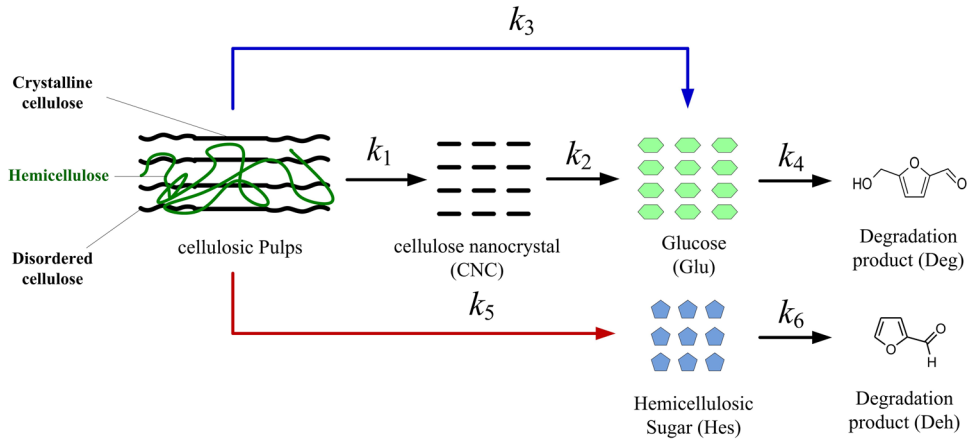


**Figure 1.** Schematic of the proposed reaction pathways for cellulosic fiber hydrolysis under strong acid conditions for the production of cellulose nanocrystals.

purchased from Sigma-Aldrich (St. Louis, MO). Bleached Kraft eucalyptus dry lap pulp was obtained from a commercial source (Aracruz Celulose S.A., Aracruz, Brazil). The Klason lignin and xylan contents of the eucalyptus pulp were 0.1 ± 0.1% and 15.5 ± 0.6%, respectively. The measured cellulose content of the pulp was 78.1 ± 1.0%; however, the normalized value of 84.4% based on mass balance was used because other components were undetectable. Cellulosic fibers were produced by soaking the dry lap pulp in water overnight and disintegrating it for 5000 revolutions at 312 rpm and 5% solids at room temperature (model 73-06-01, TMI, Ronkonkoma, New York). The pulp was then vacuum-dewatered and air-dried to approximately 5% moisture in 30% relative humidity at 26.7 °C. The air-dried pulp was used in acid hydrolysis.

**Acid Hydrolysis.** Acid hydrolysis experiments were conducted using a narrow range of acid concentrations (50–64 wt %) and temperatures (35–80 °C), but with a relatively large range of reaction times (15–240 min). These test conditions can capture the reactions of CSR and CNC along with sugars and sugar degradation products such as furfural and 5-hydroxylmethfurfural (HMF) to ensure the integrity of the kinetic model to be developed. The acid hydrolysis experiments were carried out according to the procedure described in our previous study.[9] Time-dependent data were obtained by sampling the reaction stream periodically by pipet. The reaction in each sample was immediately quenched by adding an 8-fold quantity of deionized water. After centrifugation at 9000 rpm to separate the precipitant, an aliquot of the supernatant was taken for analyses of sugars and sugar degradation products. The precipitate was dialyzed using deionized water until constant pH was reached. The suspension was centrifuged again to separate CNC from CSR.

**Determination of CNC and CSR Yields.** The yields of CNC and CSR were determined by a method involving chemical oxygen demand (COD).[9] An aliquot of CNC or CSR suspension was digested in a commercial COD test vial (Biosciences, Inc., Bethlehem, PA). Chromium consumption was determined calorimetrically at 600 nm by UV–vis spectrophotometer (Spectronic Genesys 5, Milton Roy Company, Warminster, PA). The concentrations of cellulosic suspensions were calculated from the COD data assuming that all organic materials detected originated from polymeric cellulose as $(C_6H_{10}O_5)_n$, that is, COD (mg/L) = $3410.2I^{600}$. The mass of cellulose was then calculated as $m_{C_6H_{10}O_5}$(mg/L) = COD/1.185 = $2877I^{600}$ through calibration using Avicel. The systematic error was 2.28% assuming that all organics detected originated from polymeric cellulose as $(C_6H_{10}O_5)_n$ and ignoring the fact that approximately 15% was xylan $[(C_5H_8O_4)_n]$.

**Analysis of Sugars and Degradation Products.** Sugar and its degradation products were analyzed by high-performance anion-exchange chromatography with pulsed amperometric detection (HPAEC-PAD) (Dionex ICS-3000).

**Data Processing.** The kinetic constants were obtained by nonlinear fitting of the experimental data using Matlab 6.5 software to minimize the objective function, namely, the quadratic sum of the differences between model predicted values and experimental data. The fourth-order Runge–Kutta method was used to solve the differential equations numerically.

## KINETIC MODELING

Cellulose fibers consist mainly of hemicelluloses (mainly xylan in the present study) and cellulose. It is generally believed that cellulose fibers can be divided into crystalline and noncrystalline (disordered or paracrystalline) regions. The noncrystalline cellulose regions are preferentially hydrolyzed, whereas the crystalline regions have a higher resistance to acid attack and thus a much slower hydrolysis. The hydrolysis of noncrystalline cellulose is approximately 2–30 times faster than that of crystalline cellulose.[16] As a result, rodlike cellulose nanocrystals on the order of 5–10 nm in diameter and 100 nm in length can be produced following the acid treatment of cellulose fibers.[6] A typical elemental crystal in the wood fibers has a diameter of 3–5 nm and a length of approximately 60 nm.[18] Hydrolysis of cellulose and hemicellulose to form monosaccharides such as glucose and xylose is inevitable. These sugars can be further degraded to form degradation products such as HMF and furfural.

Based on the above understanding, the reactions involved in the acid hydrolysis of cellulose fibers for CNC production can be modeled using three pathways as shown schematically in Figure 1. The first and predominant pathway, represented by rate constant $k_1$, is the hydrolysis of noncrystalline cellulose to CNCs. The CNCs can be further degraded to glucose under severe hydrolysis conditions with rate constant $k_2$. The second pathway is the direct hydrolysis of cellulose to glucose, represented by rate constant $k_3$. The basis of this pathway is that some cellulosic fraction is not directly connected to the crystalline cellulose but is rather more associated with


dx.doi.org/10.1021/ie501672m | Ind. Eng. Chem. Res. 2014, 53, 11007–11014

hemicelluloses and might have a different reaction rate in hydrolysis. The glucose resulting from the first two pathways can be further degraded to HMF, corresponding to rate constant $k_4$. The third pathway is the hydrolysis of hemicelluloses (xylan in the present study) to sugars (xylose), represented by rate constant $k_5$. The further degradation of xylose is represented by rate constant $k_6$. First-order reactions are usually used to model the hydrolysis of polysaccharides in lignocelluloses.[16,17,19] Based on Figure 1, the preparation of CNCs from bleached pulp can be described by several pseudo-first-order models.

**Xylan Hydrolysis.** It is well-known that a certain fraction of xylan is much easier (faster) to hydrolyze than others (slower).[20−22] This perhaps is due to the multilayered structure of cell walls. Therefore, under a certain hydrolysis severity, the total xylan can be phenomenologically categorized as a hydrolyzable fraction and an unhydrolyzable fraction. We can define the "potential degree of hydrolysis" for xylan ($\delta_X$, $0 \le \delta_X \le 1$) as the proportion of xylan that is hydrolyzable under the conditions employed.[16] We can thus describe xylan hydrolysis using the conventional Saeman model of first-order kinetics with respect to the remaining xylan[17,19]

$$-\frac{dX_n}{dt} = -\frac{dX_{na}}{dt} = k_5 X_{na} \tag{1}$$

where $X_{na}$ is the concentration of hydrolyzable xylan, which can be represented in terms of $\delta_X$ and the total xylan concentration ($X_n$) as

$$X_{na} = X_n - X_{n0}(1 - \delta_X) \tag{2}$$

in which $X_{n0}$ is the initial total xylan concentration (time = 0) in the pseudohomogeneous system (g/L). The rate of xylan hydrolysis can thus be expressed as

$$-\frac{dX_n}{dt} = k_5 X_n - k_5 X_{n0}(1 - \delta_X) \tag{3a}$$

The integral form of this equation is

$$X_n = X_{n0}\{1 - \delta_X[1 - \exp(-k_5 t)]\} \tag{3b}$$

The formations of xylose, $X$, and furfural, $F_{ur}$, can also be modeled using first-order kinetics as[17,23,24]

$$\frac{dX}{dt} = 1.136 k_5 X_n - k_6 X \tag{4a}$$

$$\frac{dF_{ur}}{dt} = k_6 X \tag{5a}$$

The corresponding xylose and furfural concentrations can be obtained after integration as

$$X = \frac{1.136 X_{n0}\delta_X k_5}{k_5 - k_6}[\exp(-k_6 t) - \exp(-k_5 t)] \tag{4b}$$

$$F_{ur} = \frac{1.136 X_{n0} k_5 \delta_X}{k_5 - k_6}[1 - \exp(-k_6 t)] - \frac{1.136 X_{n0} k_6 \delta_X}{k_5 - k_6}[1 - \exp(-k_5 t)] \tag{5b}$$

When the degradation of xylose can be neglected (i.e., $k_6 = 0$), the xylose concentration can be expressed as

$$X = 1.136 X_{n0}\delta_X[1 - \exp(-k_5 t)] \tag{4c}$$

**Cellulose Hydrolysis and Production of CNC.** Similarly, we can define a "degree of hydrolysis" for cellulose, $\gamma$ ($0 \le \gamma \le 1$), as the fraction of cellulose that was depolymerized to the form of glucose (DP = 1) all the way up to CNC (DP ≈ 120). Applying first-order kinetics, we modeled cellulose hydrolysis in the production of CNC as follows

$$-\frac{dC_{Cel}}{dt} = (k_1 + k_3)[C_{Cel} - C_{Cel0}(1 - \gamma)] \tag{6a}$$

$$\frac{dC_{NC}}{dt} = k_1 C_{Cel} - k_2 C_{NC} \tag{7a}$$

$$\frac{dG_{lu}}{dt} = 1.111 k_2 C_{NC} + 1.111 k_3 C_{Cel} - k_4 G_{lu} \tag{8a}$$

where $C_{Cel}$ is the concentration of cellulose remaining in the pseudohomogeneous system (g/L), $C_{Cel0}$ is the initial cellulose concentration in the pseudohomogeneous system (g/L), $C_{NC}$ is the concentration of CNC (g/L), and $G_{lu}$ is the concentration of glucose (g/L). Integration using the initial conditions $t = 0$, $C_{Cel} = C_{Cel0}$, $C_{NC} = 0$, and $G_{lu} = 0$ results in the following integral forms

$$C_{Cel} = C_{Cel0}(1 - \gamma\{1 - \exp[-(k_1 + k_3)t]\}) \tag{6b}$$

$$C_{NC} = \frac{C_{Cel0} k_1 \gamma}{k_1 + k_3 - k_2}\{\exp(-k_2 t) - \exp[-(k_1 + k_3)t]\} \tag{7b}$$

$$G_{lu} = \frac{1.111 C_{Cel0}\gamma(k_2 - k_3)(k_1 + k_3)}{(k_1 + k_3 - k_2)(k_4 - k_1 - k_3)}\{\exp(-k_4 t) - \exp[-(k_1 + k_3)t]\} + \frac{1.111 C_{Cel0}\gamma k_1 k_2}{(k_1 + k_3 - k_2)(k_4 - k_2)}[\exp(-k_2 t) - \exp(-k_4 t)] \tag{8b}$$

When the degradation of glucose can be neglected (i.e., $k_4 = 0$), the glucose concentration can be expressed as

$$G_{lu} = \frac{1.111 C_{Cel0}\gamma(k_3 - k_2)}{(k_1 + k_3 - k_2)}\{1 - \exp[-(k_1 + k_3)t]\} + \frac{1.111 C_{Cel0}\gamma k_1}{(k_1 + k_3 - k_2)}[1 - \exp(-k_2 t)] \tag{8c}$$

Then, the concentration of CSR ($C_{CSR}$, g/L) in the pseudohomogenous system can be calculated based on mass balance as

$$C_{CSR} = C_{Cel} + C_{X_n} = C_{Cel0}(1 - \gamma\{1 - \exp[-(k_1 + k_3)t]\}) + X_{n0}\{1 - \delta_X[1 - \exp(-k_5 t)]\} \tag{9}$$

The yields of CNC ($Y_{CNC}$) and CSR ($Y_{CSR}$) are defined based on the initial fiber mass concentration $C_{SR0}$ are given by

$$Y_{CNC} = \frac{C_{NC}}{C_{CSR0}} \times 100\% \tag{10}$$

$$Y_{CSR} = \frac{C_{SR}}{C_{CSR0}} \times 100\% \tag{11}$$

Thus, we can obtain the time courses of $Y_{CNC}$ and $Y_{CSR}$ as


dx.doi.org/10.1021/ie501672m | Ind. Eng. Chem. Res. 2014, 53, 11007−11014

$$Y_{CNC} = \frac{C_{Cel0}k_1\gamma}{C_{CSR0}(k_1 + k_3 - k_2)}\{\exp(-k_2 t) - \exp[-(k_1 + k_3)t]\} \times 100\% \quad (12)$$

$$Y_{CSR} = \left[\frac{C_{Cel0}}{C_{CSR0}}(1 - \gamma\{1 - \exp[-(k_1 + k_3)t]\}) + \frac{X_{n0}}{C_{SR0}}\{1 - \delta_X[1 - \exp(-k_5 t)]\}\right] \times 100\% \quad (13)$$

**Optimal Hydrolysis Time and CNC Yield.** According to eq 12, when $k_2 \neq 0$, there is an optimum time at which $Y_{CNC}$ reaches the maximum for a given acid concentration and reaction temperature. This optimum time depends on kinetic constants $k_1$, $k_2$, and $k_3$. By taking the differential calculation for eq 12, we can easily obtain that the optimum time, $t_{opt}$, as

$$t_{opt} = \frac{\ln\left(\frac{k_1 + k_3}{k_2}\right)}{k_1 + k_3 - k_2} \quad (14)$$

and the corresponding maximum CNC yield, $Y_{CNCmax}$, as

$$Y_{CNCmax} = \frac{C_{Cel0}k_1\gamma}{C_{CSR0}(k_1 + k_3)}\left(\frac{k_1 + k_3}{k_2}\right)^{k_2/(k_2 - k_1 - k_3)} \quad (15)$$

## RESULTS AND DISCUSSION

**Comparisons between Kinetic Model Predictions and Experimental Data.** Kinetic rate constants were obtained by fitting the model to the experimental yields of reaction products including CNC and CSR (Table S1, Supporting Information). Comparisons of the time-dependent experimental data with model-predicted values of the yields of CNC (eq 12) and CSR (eq 13) and the concentrations of xylose (eq 4b) and glucose (eq 8b) are shown in Figures 2–5, respectively. Good agreements were obtained, indicating that the developed models can provide good predictions of the kinetic behavior of the acid hydrolysis of cellulose fibers for CNC production.

The results also clearly indicate that the acid concentration plays a dominant role in CNC production (Figure 2). It appears that there is a maximum CNC yield for a given sulfuric acid concentration for the range of temperatures investigated. For example, the maximum CNC yield was less than 10% at an acid concentration 50 wt %. The maximum CNC yield increased to approximately 30% and 70% when the acid concentration was increased to 56 and 62 wt %, respectively. The reaction temperature and duration can affect CNC yield, but they cannot affect the maximum CNC yield for a given acid concentration. In general, the CNC yield improved with reaction time and temperature at acid concentrations below 64 wt % because of the improved hydrolysis of noncrystalline cellulose (Figure 2). However, at an acid concentration of 64 wt % or at high temperatures such as in runs (64, 45, $t$) and (62, 60, $t$), CNC degradation became important, and the CNC yield decreased under extended hydrolysis durations (Figure 2c). This behavior of CNC yield reflects the competing reactions between the first-stage cellulose depolymerization to CNC (DP ≈ 100) and CNC degradation (further depolymerization of CNC to oligomeric and monomeric sugars) in the system.

The CSR yield is dictated by the acid concentration and hydrolysis temperature when the acid concentration is below 58 wt %, as shown in Figure 3a,b. Reaction time has a limited effect

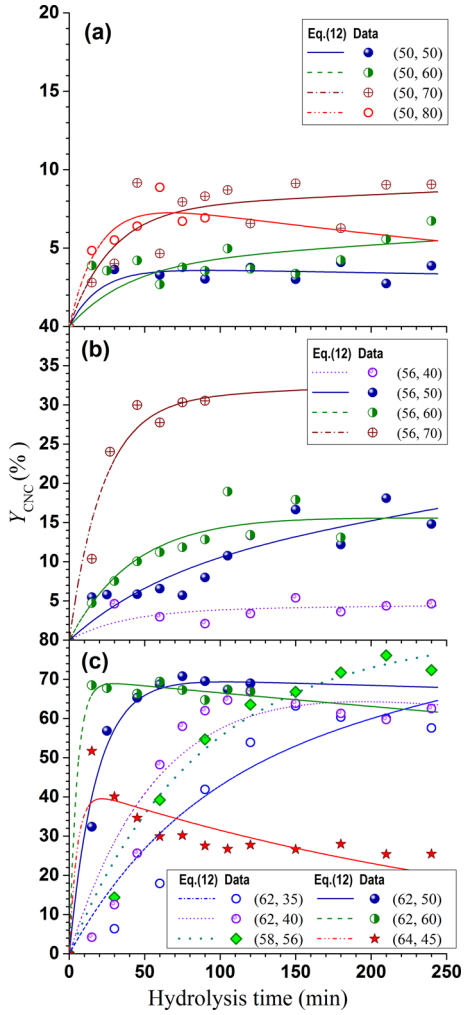


**Figure 2.** Kinetic-model-predicted time-dependent CNC yields at different temperatures in comparison with experimental data (kinetic constants from Table S1): $C_{SA}$ = (a) 50, (b) 56, and (c) $C_{SA}$ = 58–64 wt %.

except in the early stage of hydrolysis. At high acid concentrations of 58 wt % or higher, the CSR yield decreased very rapidly to near zero with time in the temperature range investigated (Figure 3c), suggesting the rapid hydrolysis of polysaccharides under strong acid conditions.

The profiles of glucose concentration were very similar to those of CNC yield (Figure 4), but with lower degradations. This suggests that pathway 1 ($k_1$) dominates pathway 2 ($k_3$) (Figure 1) and that reaction rate constant $k_4$ is negligible under most of the conditions studied. Xylan hydrolysis was fast under the conditions studied; as a result, the xylose concentration was only mildly affected by reaction temperature and acid concentration (Figure 5). After the initial rapid increase, xylose reached an asymptotic value with minimal degradation for the reaction conditions investigated (i.e., reaction rate constant $k_6$ is negligible) (Figure 5).

**Maximum CNC Yield.** For a given reaction at acid concentration $C_{SA}$ and temperature $T$ at different reaction durations, the maximum (optimum) achievable CNC yields and the corresponding optimal reaction time can be calculated using eqs 15 and 14, respectively. The calculated results were compared with experimental data. Excellent agreement was obtained, as shown in Table 1. Using $C_{SA}$ values of 58–62 wt %


dx.doi.org/10.1021/ie501672m | Ind. Eng. Chem. Res. 2014, 53, 11007–11014

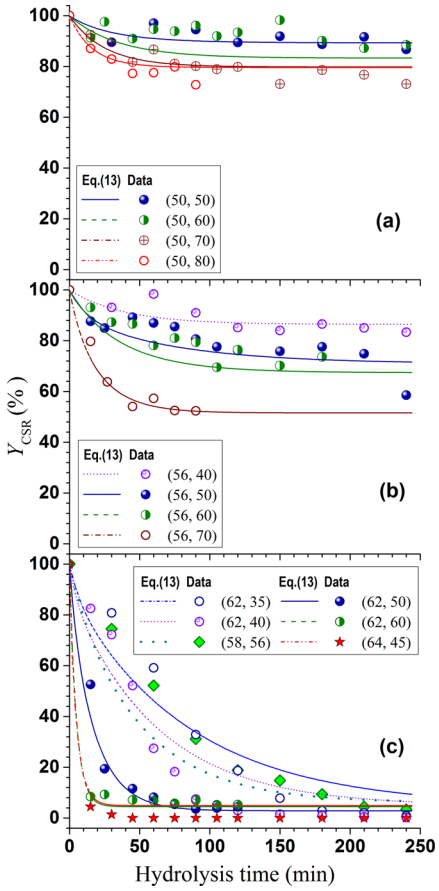


**Figure 3.** Kinetic-model-predicted time-dependent CSR yields at different temperatures in comparison with experimental data (kinetic constants from Table S1): $C_{SA}$ = (a) 50, (b) 56, and (c) 58−64 wt %.

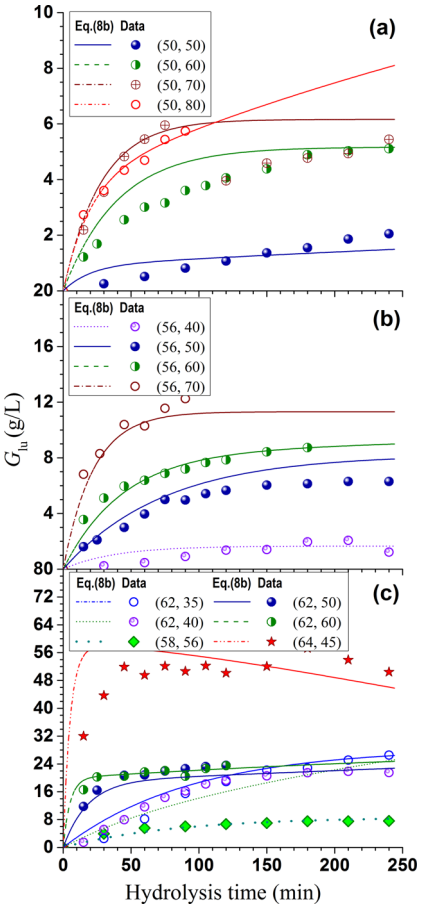


**Figure 4.** Kinetic-model-predicted time-dependent hydrolysate glucose concentration at different temperatures in comparison with experimental data (kinetic constants from Table S1): $C_{SA}$ = (a) 50, (b) 56, and (c) $C_{SA}$ = 58−64 wt %.

achieved greater maximum CNC yields than using either a lower or higher $C_{SA}$ value, because insufficient cellulose depolymerization occurred at $C_{SA}$ < 58 wt % (Figure 2a,b) and CNC degradation to glucose occurred at $C_{SA}$ = 64 wt % (Figure 2c).

To further illustrate this, we have also listed the calculated and measured CSR yield, $Y_{CSR}$, and glucose concentration, $G_{lu}$, corresponding to the reaction time that achieved the maximum CNC yield at each given $C_{SA}$ and $T$ in Table 1. Again, excellent agreement was obtained between the predicted and measured $Y_{CSR}$ and $G_{lu}$ values. Although the experiments were not exhaustive, the results clearly show that $C_{SA}$ = 58 wt % is the demarcation point below which $Y_{CSR}$ was very high (i.e., > 50%) with low $G_{lu}$, whereas $Y_{CSR}$ was very low, approximately <10%, for $C_{SA} \geq$ 58 wt %. The very high $Y_{CSR}$ > 50% and low $G_{lu}$ indicate insufficient cellulose depolymerization at low acid concentrations. The very low $Y_{CSR}$ < 10% at $C_{SA} \geq$ 58 wt % indicates that cellulose was nearly completely depolymerized under the conditions studied. This illustrates that $C_{SA} \geq$ 58 wt % is a prerequisite condition for achieving a maximum CNC yield. However, the results clearly indicate that $G_{lu}$ is high (>10 g/L) for most of the runs using $C_{SA} \geq$ 58 wt %, suggesting that CNC degradation to glucose is very difficult to avoid because of the rapid hydrolysis reactions at high acid concentrations, as also observed in literature.[9,12] The sudden changes in $Y_{CSR}$ and $G_{lu}$ at $C_{SA}$ = 58 wt % (Table 1) clearly indicate the narrow operating window in CNC production to maximize the CNC yield as reported in the literature. The very high glucose concentration of 32 g/L measured at $C_{SA}$ = 64 wt % even with only a short reaction time of 15 min at a moderate temperature of 45 °C further indicates that $C_{SA}$ = 64 wt %, as has commonly been used in the literature for CNC production, is too high to achieve a high CNC yield. The proper course of action is to use $C_{SA}$ = 58−62 wt % with a relatively longer reaction time to achieve good removal of noncrystalline and hemicellulose−cellulose linkages through cellulose depolymerization while reducing CNC degradation.

For prediction purposes, we have plotted the model-predicted yields of CNC and CSR, yield of glucose, and optimal hydrolysis time in panels a−c, respectively, of Figure 6. Because experiments were not carried out for most of the conditions plotted in Figure 6a, we could not fit the data to obtain $k$ values as we did for the predictions listed in Table 1. Rather, rate constants $k$ were determined by nonlinear regression with respect to acid concentration and temperature as described in the next section for all of the conditions plotted. Deviations of the predictions from those listed in Table 1 were observed because the $k$ values were determined differently (Figure S1a of the Supporting Information shows the difference in $k$ values between those from fitting and those from linear regression). We have also plotted the measured CNC and CSR yields at 50 °C (56 °C for 58 wt % acid, 45 °C for 64 wt % acid) in Figure 6a to further demonstrate the accuracy of the predictions. The results clearly show the demarcation point of $C_{SA}$ = 58 wt % to achieve high CNC yield and a limited effect of temperature. Temperature can affect the CNC yield at low acid


dx.doi.org/10.1021/ie501672m | Ind. Eng. Chem. Res. 2014, 53, 11007−11014

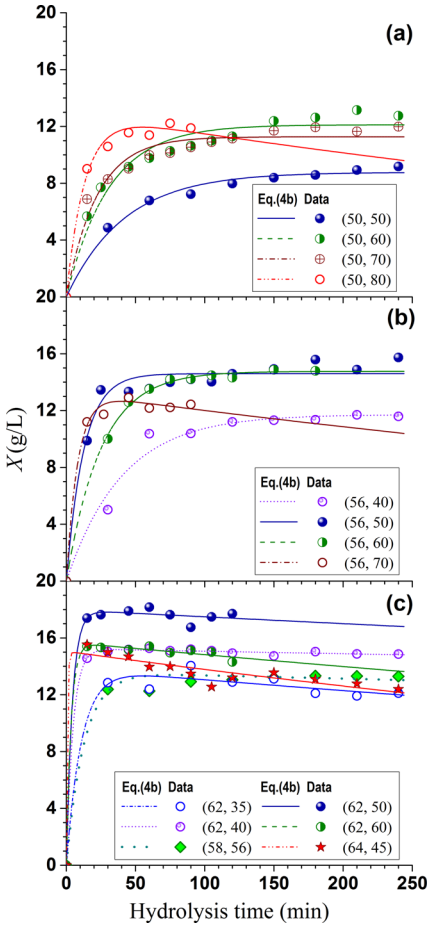


**Figure 5.** Kinetic-model-predicted time-dependent hydrolysate xylose concentration at different temperatures in comparison with experimental data (kinetic constants from Table S1): $C_{SA}$ = (a) 50, (b) 56, and (c) $C_{SA}$ = 58−64 wt %.

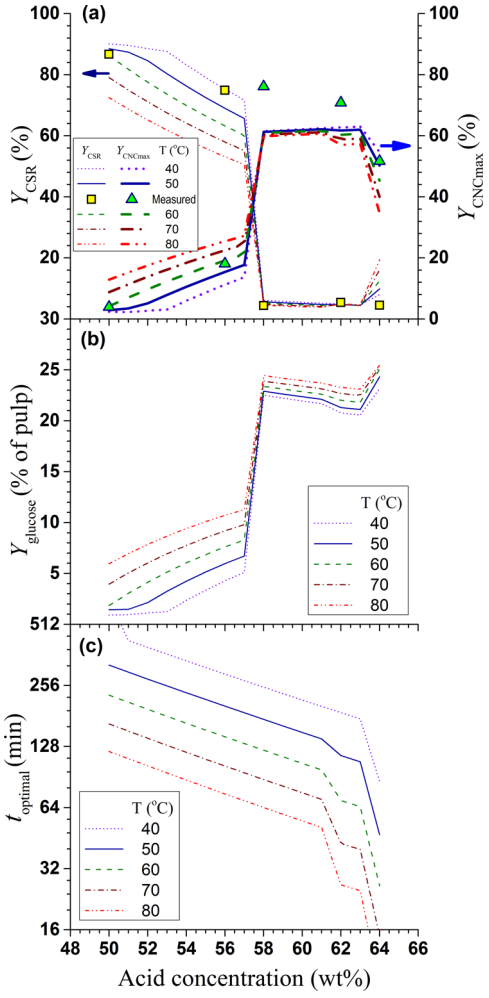


**Figure 6.** Kinetic-model-predicted maximum achievable CNC yield at different acid concentrations and reaction temperatures and corresponding CSR and glucose yield and optimal reaction time: (a) $Y_{CNCmax}$ and $Y_{CSR}$, (b) $Y_{glucose}$, and (c) $t_{optimal}$.

concentrations of $C_{SA}$ < 58 wt % but with low CNC yields of less than 30%. The CSR yield has profiles opposite those of the CNC yield (Figure 6a). Again, temperature has a limited effect on CSR yield. Cellulose degradation to glucose was apparent at $C_{SA} \geq 58$ wt % (Figure 6b). The reduction in glucose yield at $C_{SA}$ = 58−62 wt % is probably due to the errors in estimating $k_2$. The predicted optimal reaction times at various acid concentration and temperature are plotted in Figure 6c. Longer

**Table 1. Comparisons of Predicted Maximum CNC Yield and the Corresponding CSR Yield and Glucose Concentrations with Experimental Data**

| $C_{SA}$ | | | | | $Y_{CNCmax}$ (%) | | $Y_{CSR}$ (%) | | $G_{lu}$ (g/L) | |
|---|---|---|---|---|---|---|---|---|---|---|
| (mol/L) | (wt %) | $T$ (°C) | $t_{opt}$ (min) (eq 14) | $t_{exp}$ (min) | eq 15 | expt | eq 13 | expt | eq 8b | expt |
| 7.097 | 50 | 50 | 239 | 240 | 2.9 | 3.9 | 89.3 | 86.7 | 1.7 | 2.0 |
| 7.097 | 50 | 60 | 229 | 240 | 4.2 | 6.7 | 83.3 | 88.5 | 2.5 | 5.1 |
| 7.097 | 50 | 70 | 294 | 240 | 8.9 | 9.1 | 79.8 | 73.1 | 5.3 | 5.4 |
| 7.097 | 50 | 80 | 82 | 90 | 12.2 | 6.9 | 79.8 | 72.8 | 8.0 | 5.7 |
| 8.295 | 56 | 40 | 291 | 240 | 11.2 | 5.4 | 86.4 | 84.0 | 5.5 | 1.4 |
| 8.295 | 56 | 50 | 202 | 210 | 15.4 | 18.1 | 72.1 | 74.9 | 7.9 | 6.5 |
| 8.295 | 56 | 60 | 143 | 150 | 19.2 | 18.9 | 68.2 | 69.5 | 10.2 | 7.7 |
| 8.295 | 56 | 70 | 103 | 90 | 22.5 | 30.5 | 69.6 | 52.4 | 12.5 | 12.2 |
| 8.715 | 58 | 56 | 205 | 210 | 65.7 | 76.1 | 7.4 | 4.4 | 7.9 | 7.5 |
| 9.589 | 62 | 35 | 228 | 180 | 62.8 | 63.3 | 10.3 | 2.8 | 27.7 | 32.6 |
| 9.589 | 62 | 40 | 195 | 120 | 64.2 | 67.1 | 8.4 | 3.0 | 22.0 | 19.3 |
| 9.589 | 62 | 50 | 101 | 75 | 69.2 | 70.8 | 3.1 | 5.4 | 20.4 | 22.0 |
| 9.589 | 62 | 60 | 30 | 60 | 68.9 | 69.4 | 4.7 | 6.8 | 20.6 | 21.7 |
| 10.043 | 64 | 45 | 64 | 15 | 52.5 | 51.7 | 4.9 | 4.5 | 55.0 | 32.0 |


dx.doi.org/10.1021/ie501672m | Ind. Eng. Chem. Res. 2014, 53, 11007−11014

reaction times are needed when hydrolysis is conducted at low temperatures. Therefore, a moderate temperature of 50−60 °C is preferred to reduce the reaction time even though temperature has a minimal effect on CNC yield (Figure 6a).

**Reaction Rate Constants.** The regression-obtained rate constants $k$ can be correlated with $T$ and $C_{SA}$ using the expanded Arrhenius equation

$$k = k_0 \exp\left(-\frac{E_a}{RT}\right) {C_{SA}}^m \tag{16}$$

where $k_0$ and $E_a$ are the pre-exponential factor and activation energy, respectively, and $m$ is the reaction order with respect to acid concentration. Similarly, this equation can be expressed as

$$\ln k = \ln k_0 - \frac{E_a}{R}\frac{1}{T} + m \ln C_{SA} \tag{17}$$

where $k_0$, $E_a$, and $m$ can be determined by plotting ln $k$ with $1/T$ and $C_{SA}$, and the results are listed in Table 2.

**Table 2. Kinetic Constants for Predicting Rate Constants $k$ and Degrees of Hydrolyzable Cellulose and Xylan**

| $k$ or $\delta_X$ | $k_0$ or $B$ | $E_a$ (kJ/mol) or $\varepsilon$ | $m$ or $\beta$ | conditions |
|---|---|---|---|---|
| $\gamma$ | 60.8259 | 0.1314 | 1.9752 | 50% < $C_{SA}$ < 58%, 308 K < $T$ < 353 K |
| $k_1$ | 4.8059 | 36.353 | 3.8157 | 50% < $C_{SA}$ < 64%, 308 K < $T$ < 353 K |
| $k_3$ | 24.1186 | 40.222 | 3.2566 | 50% < $C_{SA}$ < 64%, 308 K < $T$ < 353 K |
| $\delta_X$ | 46.3115 | 0.0974 | 2.1853 | 50% < $C_{SA}$ < 64%, 308 K < $T$ < 353 K |
| $k_5$ | 0.0010 | 31.442 | 7.5119 | 50% < $C_{SA}$ < 64%, 308 K < $T$ < 353 K |

Therefore, the kinetic constants in the models can be expressed using the following equations

$$k_1 = 4.8059 \exp\left(-\frac{36353}{RT}\right) {C_{SA}}^{3.8157} \tag{18a}$$

$$k_3 = 24.1186 \exp\left(-\frac{40222}{RT}\right) {C_{SA}}^{3.2566} \tag{18b}$$

$$k_5 = 0.0010 \exp\left(-\frac{31442}{RT}\right) {C_{SA}}^{7.5119} \tag{18c}$$

Because not enough data were obtained for the CNC hydrolysis and sugar degradation reactions, the relationships for $k_2$, $k_4$, and $k_6$ were not established. The rate constants $k_1$−$k_3$ predicted using eqs 18a−18c were compared with those obtained by fitting the experimental data, as shown in Figure S1a (Supporting Information). The agreement was found to be good in general. Large discrepancies were observed for a few data points with low $k$ values, especially $k_1$ and $k_3$, which were less than 0.1 as a result of experimental and mathematical difficulties.

The rate constant for xylose formation ($k_5$) was found to be 1−2 orders of magnitude larger than that for glucose formation ($k_3$). Similar results were also reported when dilute acid was used to hydrolyze lignocellulosic biomass.[16,26,27] The degradations of xylose and glucose were negligible in most cases. Significant degradations were observed only under severe condition such as $C_{SA}$ > 62% or $T$ > 60 °C. The rate constant for xylan hydrolysis was found to be 4 orders of magnitude greater than that for xylose degradation, and the rate constant for cellulose hydrolysis was about 2 orders of magnitude greater than that for glucose degradation. The hydrolysis of CNCs is not significant in most cases, except at acid concentrations of 64 wt % or higher.

As shown in Table 2, cellulose hydrolysis to form glucose had the highest activation energy, whereas xylan hydrolysis had the lowest. Both activation energies were much lower than those for the dilute acid hydrolysis of lignocelluloses,[16,17] indicating that strong acid facilitates the hydrolysis of cellulose and xylan at low temperatures.

**Degrees of Hydrolyzable Cellulose and Xylan.** The degrees of hydrolyzable cellulose, $\gamma$, and xylan, $\delta_X$, are functions of reaction severity, that is, sulfuric acid concentration $C_{SA}$ and temperature $T$. Based on the combined severity factor concept,[25] we can establish a temperature-related severity

$$R_0 = \exp\left(\frac{T' - T_r}{14.75}\right) \tag{19}$$

where $T'$ is the temperature in °C and $T_r$ is a reference temperature. In this work, we chose $T_r$ = 25 °C, at which the degradation of CNC should be low. Considering the effect of sulfuric acid, a "combined severity factor" ($R$) is defined as

$$R = {C_{SA}}^n \exp\left(\frac{T' - T_r}{14.75}\right) = {C_{SA}}^n R_0 \tag{20}$$

where the exponent $n$ represents the strong acid dependence of the hydrolysis reactions under strong acid conditions. When $R$ reaches a certain critical severity ($RC$) contributed by high $C_{SA}$ or $T$, $\gamma$ or $\delta_X$ tends toward 1, that is, $\lim_{R\to R_C} \gamma = 1$ and $\lim_{R\to R_C} \delta_X = 1$. Therefore, for $R < R_C$ (corresponding to $C_{SA} < C_{SAC}$ or $T < T_C$), the relationship between $\gamma$ or $\delta_X$ and $R$ can thus be proposed as

$$\gamma \text{ or } \delta_X = 1 - \frac{B}{R^\alpha} = 1 - \frac{B}{{C_{SA}}^\beta {R_0}^\varepsilon} \tag{21}$$

where $B$ is a constant and $\beta$ and $\varepsilon$ are corresponding exponents that reflect the impacts of sulfuric acid and temperature, respectively, on $\gamma$ or $\delta_X$. These equations can also be expressed as

$$\ln \frac{1}{1 - \gamma \text{ (or } \delta_X)} = -\ln B + \beta \ln C_{SA} + \varepsilon \ln R_0 \tag{22}$$

Therefore, the parameters $B$, $\beta$, and $\varepsilon$ can be determined by plotting $\ln[1/(1-\gamma)]$ or $\ln[1/(1-\delta_X)]$ versus $C_{SA}$ and $R_0$

$$\gamma = 1 - \frac{60.8259}{{C_{SA}}^{1.9752} {R_0}^{0.1314}} \tag{23a}$$

$$\delta_X = 1 - \frac{46.3115}{{C_{SA}}^{2.1853} {R_0}^{0.0974}} \tag{23b}$$

As discussed previously, an acid concentration of 58 wt % is the demarcation point above which cellulosic fibers can be completely dissolved; therefore, $\gamma = 1$ when $C_{SA} \geq 58\%$, in which case eq 23a is no longer valid.

The degrees of hydrolyzable cellulose and xylan predicted using eqs 23a and 23b were compared with those determined by fitting the experimental data. Excellent agreement was obtained (Figure S1b, Supporting Information), suggesting that the approach employed to derive eqs 23a and 23b using the combined severity factor defined in eq 20 is valid.


dx.doi.org/10.1021/ie501672m | Ind. Eng. Chem. Res. 2014, 53, 11007−11014

## CONCLUSIONS

Reaction conditions must be well controlled to maximize the CNC yield and eliminate the degradation of cellulose fibers to sugars. The solubilization of cellulosic fibers under strong acid conditions can be simplified as three phenomenological parallel reactions: depolymerization of cellulose to form CNCs, hydrolysis of certain noncrystalline regions of cellulose to form glucose, and hydrolysis of xylan to form xylose. Hydrolysis of CNCs can occur to release glucose. Glucose and xylose can be degraded to form HMF and furfural, respectively, under more severe conditions.

CNC yield is dictated by two key processes: (1) cellulose depolymerization under low-severity conditions such as acid concentrations of <58 wt % and (2) CNC degradation at very high-severity conditions such as acid concentrations of ≥64 wt %. For bleached kraft eucalyptus pulp, a sulfuric acid concentration between 58 and 62 wt % is preferred at a moderate temperature of 50−60 °C to maximize CNC yield with a reaction time between 30 and 180 min to reduce cellulose loss to sugars. Near-zero cellulose loss to sugars and sugar degradation products can be achieved using sulfuric acid at 58 wt % and approximately 55 °C.

## ASSOCIATED CONTENT

### Supporting Information

Reaction rate constants obtained from nonlinear regression of the experimental data (Table S1). Comparisons of reaction rate constants and degrees of hydrolyzable cellulose and xylan between those obtained from fitting experimental data and predictions for correlations (Figure S1). This material is available free of charge via the Internet at http://pubs.acs.org.

## AUTHOR INFORMATION

### Corresponding Authors

*E-mail: zhaoxb@mail.tsinghua.edu.cn (X.Z.).
*E-mail: jzhu@fs.fed.us. Tel.: 608-231-9520 (J.Y.Z.).

### Notes

The authors declare no competing financial interest.

## ACKNOWLEDGMENTS

This work was conducted while Q.W. was a visiting student and X.Z. was a Sr. Visiting Scientist at the Forest Products Laboratory (FPL), U.S. Forest Service, Madison, WI, and on official government time of J.Y.Z. This work was supported by the U.S. Forest Service. Financial support included a USDA Agriculture and Food Research Initiative (AFRI) Competitive Grant (No. 2011-67009-20056); the Chinese Scholarship Council (CSC); and a USDA Agriculture and Food Research Initiative Competitive Grant (No. 2011-68005-30416), through the Northwest Advanced Renewables Alliance (NARA). The funding from these programs made the visiting appointments of Q.W. and X.Z. at FPL possible.

## REFERENCES

(1) Šturcová, A.; Davies, G. R.; Eichhorn, S. J. Elastic Modulus and Stress-Transfer Properties of Tunicate Cellulose Whiskers. *Biomacromolecules* **2005**, *6*, 1055−1061.
(2) Mark, R. E. *Cell Wall Mechanics of Tracheids*; Yale University Press: New Haven, CT, 1967; p 119.
(3) Revol, J.-F.; Godbout, L.; Dong, X.-M.; Gray, D. G.; Chanzy, H.; Maret, G. Chiral nematic suspensions of cellulose crystallites; phase separation and magnetic field orientation. *Liq. Cryst.* **1994**, *16*, 127−134.
(4) Roman, M.; Gray, D. G. Parabolic Focal Conics in Self-Assembled Solid Films of Cellulose Nanocrystals. *Langmuir* **2005**, *21*, 5555−5561.
(5) Dong, X. M.; Gray, D. G. Induced Circular Dichroism of Isotropic and Magnetically-Oriented Chiral Nematic Suspensions of Cellulose Crystallites. *Langmuir* **1997**, *13*, 3029−3034.
(6) Habibi, Y.; Lucia, L.; Rojas, O. Cellulose Nanocrystals: Chemistry, Self-Assembly, and Applications. *Chem. Rev.* **2010**, *110*, 3479−3500.
(7) Klemm, D.; Kramer, F.; Moritz, S.; Lindstrom, T.; Ankerfors, M.; Gray, D.; Dorris, A. Nanocelluloses: A New Family of Nature-Based Materials. *Angew. Chem., Int. Ed.* **2011**, *50*, 5438−5466.
(8) Moon, R. J.; Martini, A.; Nairn, J.; Simonsen, J.; Youngblood, J. Cellulose nanomaterials review: Structure, properties and nanocomposites. *Chem. Soc. Rev.* **2011**, *40*, 3941−3994.
(9) Wang, Q. Q.; Zhu, J. Y.; Reiner, R. S.; Verrill, S. P.; Baxa, U.; McNeil, S. E. Approaching zero cellulose loss in cellulose nanocrystal (CNC) production: Recovery and characterization of cellulosic solid residues (CSR) and CNC. *Cellulose* **2012**, *19*, 2033−2047.
(10) Mukherjee, S. M.; Woods, H. J. X-ray and electron microscope studies of the degradation of cellulose by sulphuric acid. *Biochim. Biophys. Acta* **1953**, *10*, 499−511.
(11) Nickerson, R. F.; Habrle, J. A. Cellulose Intercrystalline Structure. *Ind. Eng. Chem.* **1947**, *39*, 1507−1512.
(12) Hamad, W. Y.; Hu, T. Q. Structure−process−yield interrelations in nanocrystalline cellulose extraction. *Can. J. Chem. Eng.* **2010**, *88*, 392−402.
(13) Bondeson, D.; A, M.; Oksman, K. Optimization of the isolation of manocrystals from microcrystalline cellulose by acid hydrolysis. *Cellulose* **2006**, *13*, 171−180.
(14) Beck-Candanedo, S.; Roman, M.; Gray, D. G. Effect of Reaction Conditions on the Properties and Behavior of Wood Cellulose Nanocrystal Suspensions. *Biomacromolecules* **2006**, *6*, 1048−1054.
(15) Wang, Q. Q.; Zhu, J. Y.; Considine, J. M. Strong and Optically Transparent Films Prepared Using Cellulosic Solid Residue (CSR) Recovered from Cellulose Nanocrystals (CNC) Production Waste Stream. *ACS Appl. Mater. Interfaces* **2013**, *5*, 2527−2534.
(16) Zhao, X.; Zhou, Y.; Liu, D. Kinetic model for glycan hydrolysis and formation of monosaccharides during dilute acid hydrolysis of sugarcane bagasse. *Bioresour. Technol.* **2012**, *105*, 160−168.
(17) Saeman, J. F. Kinetics of Wood Saccharification: Hydrolysis of Cellulose and Decomposition of Sugars in Dilute Acid at High Temperature. *Ind. Eng. Chem.* **1945**, *37*, 43−52.
(18) Stamm, A. J. *Wood and Cellulose Science*; The Ronald Press Company: New York, 1964.
(19) Springer, E. L. Hydrolysis of Aspenwood xylan with aqueous solutions of hydrochloric acid. *TAPPI J.* **1966**, *49*, 102−106.
(20) Kobayashi, T.; Sakai, Y. Hydrolysis rate of pentosan of hardwood in dilute sulfuric acid. *Bull. Agric. Chem. Soc. Jpn.* **1956**, *20*, 1−7.
(21) Maloney, M. T.; Chapman, T. W.; Baker, A. J. Dilute acid hydrolysis of paper birch: Kinetics studies of xylan and acetyl-group hydrolysis. *Biotechnol. Bioeng.* **1985**, *27*, 355−361.
(22) Zhu, W.; Houtman, C. J.; Zhu, J. Y.; Gleisner, R.; Chen, K. F. Quantitative predictions of bioconversion of aspen by dilute acid and SPORL pretreatments using a unified combined hydrolysis factor (CHF). *Process Biochem.* **2012**, *47*, 785−791.
(23) Xiang, Q.; Lee, Y. Y.; Torget, R. W. Kinetics of glucose decomposition during dilute-acid hydrolysis of lignocellulosic biomass. *Appl. Biochem. Biotechnol.* **2004**, *113−16*, 1127−1138.
(24) Zhang, C.; Houtman, C. J.; Zhu, J. Y. Using low temperature to balance enzymatic saccharification and furan formation in SPORL pretreatment of Douglas fir. *Process Biochem.* **2014**, *49*, 466−473.
(25) Chum, H. L.; Johnson, D. K.; Black, S. K.; Overend, R. P. Pretreatment-catalyst effects of the combined severity parameter. *Appl. Biochem. Biotechnol.* **1990**, *24/25*, 1−14.
(26) Aguilar, R.; Ramirez, J. A.; Garrote, G.; Vazquez, M. Kinetic study of the acid hydrolysis of sugar cane bagasse. *J. Food Eng.* **2002**, *55*, 309−318.
(27) Guerra-Rodriguez, E.; Portilla-Rivera, O. M.; Jarquin-Enriquez, L.; Ramirez, J. A.; Vazquez, M. Acid hydrolysis of wheat straw: A kinetic study. *Biomass Bioenergy* **2012**, *36*, 346−355.